

Accepted Manuscript

Synthesis, structure-activity relationship and biological evaluation of 2,4,5-trisubstituted pyrimidine CDK inhibitors as potential anti-tumour agents

Hao Shao, Shenhua Shi, David W. Foley, Frankie Lam, Abdullah Y. Abbas, Xiangrui Liu, Shiliang Huang, Xiangrui Jiang, Nadiah Baharin, Peter M. Fischer, Shudong Wang

PII: S0223-5234(13)00572-2

DOI: [10.1016/j.ejmech.2013.08.052](https://doi.org/10.1016/j.ejmech.2013.08.052)

Reference: EJMECH 6402

To appear in: *European Journal of Medicinal Chemistry*

Received Date: 18 June 2013

Revised Date: 27 July 2013

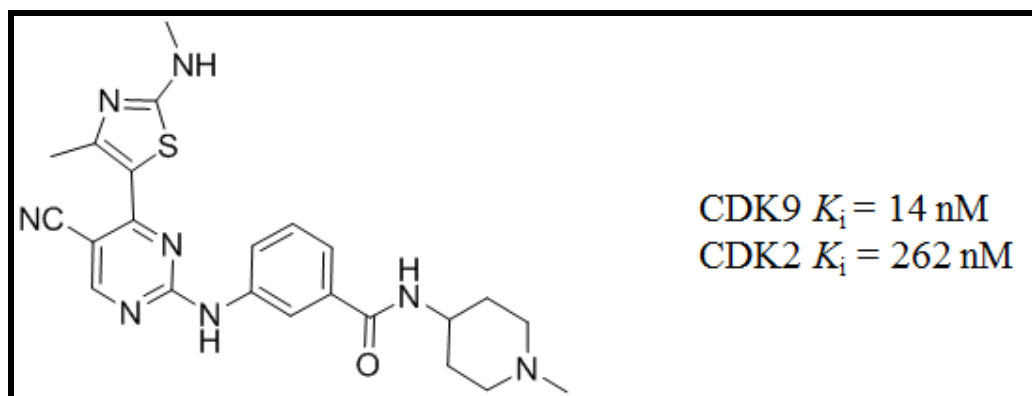
Accepted Date: 21 August 2013

Please cite this article as: H. Shao, S. Shi, D.W. Foley, F. Lam, A.Y. Abbas, X. Liu, S. Huang, X. Jiang, N. Baharin, P.M. Fischer, S. Wang, Synthesis, structure-activity relationship and biological evaluation of 2,4,5-trisubstituted pyrimidine CDK inhibitors as potential anti-tumour agents, *European Journal of Medicinal Chemistry* (2013), doi: 10.1016/j.ejmech.2013.08.052.

This is a PDF file of an unedited manuscript that has been accepted for publication. As a service to our customers we are providing this early version of the manuscript. The manuscript will undergo copyediting, typesetting, and review of the resulting proof before it is published in its final form. Please note that during the production process errors may be discovered which could affect the content, and all legal disclaimers that apply to the journal pertain.



Graphical abstract



**Synthesis, structure-activity relationship and biological evaluation of
2,4,5-trisubstituted pyrimidine CDK inhibitors as potential anti-tumour
agents**

Hao Shao^a, Shenhua Shi^a, David W. Foley^a, Frankie Lam^{a,b}, Abdullah Y. Abbas^a, Xiangrui Liu^a, Shiliang Huang^a, Xiangrui Jiang^a, Nadiyah Baharin^a, Peter M. Fischer^a and Shudong Wang^{a,b,*}

^aSchool of Pharmacy and Centre for Biomolecular Sciences, University of Nottingham, Nottingham NG7 2RD, UK

^bSansom Institute for Health Research, School of Pharmacy and Medical Sciences, University of South Australia, Adelaide SA 5001, Australia

*Corresponding author. Sansom Institute for Health Research, School of Pharmacy and Medical Sciences, University of South Australia, Adelaide SA 5001, Australia.

Tel.: +61 883022372; fax: +61 883021087.

E-mail address: shudong.wang@unisa.edu.au (S. Wang).

Keywords: CDK9 inhibitors, inhibitor design, RNA polymerase II, Mcl-1 anti-apoptotic proteins, anti-cancer drug discovery.

ABSTRACT

A series of 2, 4, 5-trisubstituted pyrimidines have been synthesized and characterised, which exhibited potent CDK inhibition and anti-proliferative activities. The structure-activity relationship is analysed and a rationale for CDK9 selectivity is discussed. Compound **9s**, possessing appreciable selectivity for CDK9 over other CDKs, is capable of activating caspase 3, reducing the level of Mcl-1 anti-apoptotic protein, and inducing cancer cell apoptosis.

1. Introduction

Cyclin-dependent kinases (CDKs) are a family of serine threonine protein kinases involved in cell cycle and transcription. The family includes two major groups: cell cycle CDKs and transcriptional CDKs. Cyclin D-CDK4/6 and cyclin E-CDK2 promote the cell cycle transition from G1 to S phase by sequentially phosphorylating the retinoblastoma protein (Rb). Cyclin A-CDK1/2 and Cyclin B-CDK1 are crucial for progression of S-phase and G2/M transition, respectively [1, 2]. Development of CDK inhibitors initially focussed on cell-cycle CDKs, but this approach was challenged when functional redundancy amongst these CDKs was demonstrated. Cancer cells depleted of CDK1, CDK2 or CDK4/6 continue to proliferate and CDK2 or CDK4/6 knockout mice are viable [3-7]. The recent advancement of the selective CDK4/6 inhibitor PD-0332991 into Phase III clinical trial for treatment of oestrogen receptor (ER)-positive breast cancer however, has revived interest in cell cycle inhibitors. These inhibitors may be useful therapeutically if administered to appropriate patients [8, 9].

The second group of CDKs, mainly CDK7 and CDK9, are involved in transcription regulation through the sequential phosphorylation of the carboxyl terminal domain (CTD) hepta peptide repeat of the largest subunit of RNA polymerase II. The general transcription factor IIIH, a complex of cyclin H-CDK7 and the RING-finger protein MAT1, phosphorylates Ser5 of the CTD to initiate transcription [10, 11]. After initiation of transcription, positive transcription elongation factor b (P-TEFb), consisting of cyclin T-CDK9, first phosphorylates the SpT5 (p160) subunit of DRB-sensitivity-inducing factor (DSIF) and the negative elongation factor (NELF), followed by Ser2, and occasionally Ser5, on the CTD of RNAP II to promote productive RNA elongation [12-14]. CDK9 regulates the transcription, while CDK7 is also known as a CDK-activating kinase (CAK) and is involved in the cell cycle [10].

CDKs have been pursued as anti-cancer drug targets for more than a decade and a number of compounds have been subjected to clinical trials. The first generation of pan-CDKs inhibitors, such as flavopiridol and *R*-Roscovitine (seliciclib), are also potent CDK9 inhibitors and their anti-tumour activity has been attributed to down-regulation of CDK9-mediated anti-apoptotic proteins, especially Mcl-1 [15-17]. An analogue of *R*-Roscovitine, CR-8, also reduces the level of Mcl-1 and induces apoptosis through inhibition of CDK9 in neuroblastoma cells [18]. Dinaciclib, a selective inhibitor of CDK 1, 2 and 9, has been recently advanced into Phase III clinical studies for the treatment of refractory chronic lymphocytic leukaemia (CLL), all of which validates continued interest in CDK9 as a therapeutic target in cancer [19]. Our research into CDK inhibitors has identified several classes of chemical compounds [20-23]. Here, we report the design, synthesis and biological evaluation of a novel class of 2,4,5-trisubstituted pyrimidine CDK inhibitors as potential anti-cancer agents.

2. Chemistry

2.1. Synthesis

The general chemistry for the synthesis of 2,4,5-trisubstituted pyrimidine compounds was adapted from the methods reported previously [20, 24] and is outlined in **Scheme 1**. Briefly, treatment of appropriate thioureas **1** with 3-chloro-2,4-pentadione resulted in 5-acetylthiazoles **2**, followed by heating in *N,N*-dimethylformamide dimethyl acetal (DMF-DMA) to get the corresponding enaminones **3**. The fluorinated enaminones **4a** and **4b** were obtained from **3** by treatment with selectfluor in methanol. The synthesis of *tert*-butyl 5-(2-cyanoacetyl)-4-methylthiazol-2-yl(methyl)carbamate **4c** started from ethyl-4-methyl-2-(methylamino)thiazole-5-carboxylate **5**, which can be easily formed through cyclization of

ethyl 2-chloro-3-oxobutanoate and 1-methylthiourea. Following Boc protection and treatment of **6** with acetonitrile in the presence of LDA afforded 5-(2-cyanoacetyl)-thiazole **7** in high yield. Enaminone **4c** was obtained by heating **7** in DMF-DMA. The guanidine **8** was prepared by heating aniline and cyanamide in the presence of trimethylsilyl chloride. The final compounds **9a-s** were obtained by treating **4a-c** and corresponding guanidines **8** under microwave-aided reaction conditions.

2.2. Structure-activity relationship analysis

We observed previously that 2C-methylamino group of the thiazole formed hydrogen bonds in the co-crystal structures of CDK9, which was not always the case in CDK2 [25]. We therefore designed and synthesised several analogues to probe the effect on potency and selectivity. All compounds were tested against CDK1, 2, 7 and 9, as well as two human tumour cell lines (**Table 1**). The primary amino analogues, i.e. **9a**, **9b** and **9d**, are more potent in cells compared with the corresponding methylamino analogues, but no CDK9 selectivity advantage is observed.

Compound **9a**, containing a sulfonamide at the *meta*-position of aniline, inhibits CDK9, CDK1 and CDK2 potently with single-digit K_i , ranging from 3-7 nM. Replacing the sulfonamide with bulkier functional groups resulted in **9b** ($R^3 = m$ -4-acetylpiperazin-1-yl) and **9c** ($R^3 = m$ -4-methylpiperazin-1-yl), showing 4-6 fold and 7-fold selectivity for CDK9 over CDK1 and CDK2 respectively. Compound **9b** demonstrated the best selectivity over CDK7, 145-fold, of this series of analogues.

Our previous studies has demonstrated that the CDK9 ATP binding pocket is more malleable and can accommodate larger functional groups on the aniline ring when compared with CDK2 [25]. A series of analogues with increased flexibility at the *meta* position of the

aniline were thus designed and synthesized. Not only do the sulfonyl and carbonyl linkages chosen allow for different conformations to be sampled, they may also have beneficial effects on the drug-like properties of the compounds. Compound **9e** ($R^1 = \text{NHMe}$, $R^2 = \text{CN}$ and $R^3 = \text{SO}_2\text{Me}$) is a potent CDK9 inhibitor, but shows only modest selectivity for CDK9. Alkylsulfone analogue **9f** ($R^2 = \text{F}$, $R^3 = \text{SO}_2\text{NH}(\text{CH}_2)_2\text{OMe}$) and **9g** ($R^2 = \text{CN}$, $R^3 = \text{SO}_2\text{NH}(\text{CH}_2)_2\text{OMe}$) did not offer improvement in selectivity when compared to **9e**; a considerable enhancement in CDK9 inhibitory potency was however observed with **9g**, indicating tolerance of methoxyethyl benzenesulfonamide, and that 5C-fluoro is superior to 5C-cyano for CDK9 inhibition. Compound **9h** ($R^2 = \text{CN}$, $R^3 = m\text{-SO}_2\text{-morpholin-4-yl}$), with a bulkier morpholinosulfonamide at the *meta*-position of aniline, enhanced the selectivity for CDK9 over other CDKs when compared to **9e-g**. Introduction of a methyl group at the *para*-position while keeping the *meta*-morpholinosulfonamide resulted in compounds **9i-j**, which showed a further improvement in selectivity for CDK9 over CDK1 and CDK2, however, the selectivity over CDK7 decreased dramatically. This is consistent with the SAR reported for another series of CDK9 inhibitors [26]. The C5-fluoro and C5-cyano substituted analogues were more potent than the corresponding C5-unsubstituted analogues, as evidenced by compounds **9j** and **9i**, **9m** and **9l**. This may be due to electronic effects of the C5-fluoro and C5-cyano enhancing binding to the hinge region of CDK9. Compound **9k** ($R^1 = \text{NHMe}$, $R^2 = \text{CN}$, $R^3 = m\text{-SO}_2\text{-4-methylpiperazin-1-yl}$) was the most potent CDK7 inhibitor in this series with a K_i value of 24 nM. Compounds **9l-o** exhibited a similar CDK inhibitory profile, but **9m** ($R^2 = \text{CN}$, $R^3 = m\text{-CO-morpholine}$) offered ~ 43-fold selectivity for CDK9 over CDK7, albeit with slightly reduced potency. Analogue **9p** ($R^2 = \text{CN}$, $R^3 = m\text{-CO-4-methylpiperazin-1-yl}$, *o*-Cl) containing an additional chloro at the *ortho*-position of aniline showed dramatically reduced kinase and cellular potency, although it showed a very interesting

kinase selectivity profile for CDK9 over CDK1, CDK2 and CDK7. Modification of keto-*N*-(1-methylpiperidin-4-yl) at the *para* or *meta*-position resulted in inhibitors **9q-s**. **9s** ($R^2 = \text{CN}$, $R^3 = m\text{-CO-}N\text{-1-methylpiperidin-4-yl}$) exhibited a better selectivity profile for CDK9 versus CDK1 and CDK2 compared to **9r** ($R^2 = \text{CN}$, $R^3 = p\text{-CO-}N\text{-1-methylpiperidin-4-yl}$) and **9q** ($R^2 = \text{F}$, $R^3 = m\text{-CO-}N\text{-1-methylpiperidin-4-yl}$). Interestingly, **9s** was also a more potent CDK9 inhibitor than its corresponding C5-fluoro analogue **9q**.

2.3. Molecular docking

Molecular docking experiments were carried out in order to rationalise the observed selectivity differences between **9q** and **9s**. We recently solved the crystal structures of several members of this series bound to CDK9 and CDK2 [25]. We revealed that ligand binding could induce significant CDK9 structural changes *via* a downward movement of the glycine rich loop. This plasticity, absent in CDK2, may be critical for obtaining CDK9 specificity. We therefore used crystal structures representative of the open [PDB ID: 4BCF] and closed [PDB ID: 4BCG] forms of CDK9 as well as a comparable [PDB ID: 4BCP] CDK2 crystal structure to investigate the binding models of **9q** and **9s** in an attempt to rationalise the selectivity profiles observed.

Upon docking the compounds into the closed CDK9 structure [4BCG], both **9q** and **9s** adopted an identical conformation (Figure 1A and 1B), giving Chemgauss 4 scores of -13.2131 and -12.6736, respectively. When the open CDK9 structure [4BCF] was used for the docking study, as shown in Figure 1C, **9s** adopted a conformation similar to that of the **9s**/4BCG, resulting in Chemgauss 4 score of -13.5206. In contrast, **9q** exhibited a rather different binding conformation than **9q**/4BCG, which resulted in a lower Chemgauss 4 score of -15.0470 (Figure 1D). This energy difference was driven by the formation of an internal

hydrogen bond between the 4N-methylpiperidine and the 2C-NH-methylthiazole. We have shown that the ability of CDK9 to accommodate a closed conformation around these ligands is crucial for selectivity [23]. **9q** appears to prefer the open conformation of CDK9 and this preference may explain the reduced selectivity when compared to **9s**.

In the structure of CDK2 (PDB ID: 4BCP) **9q** adopted a conformation such that it became involved in water-mediated hydrogen bonds connecting Asn132 and Asp145 (Figure 1E). No such hydrogen-bonding network was observed when **9s** was docked into 4BCP which may also rationalise the increased affinity for CDK2 of **9q** when compared to **9s**.

3. Pharmacology

3.1. Cytotoxicity in human tumour cell lines

The anti-proliferative activity of each compound was assessed against human HCT-116 colorectal carcinoma and MCF-7 breast cancer cells. Determination of proliferation using the MTT assay showed that growth was inhibited for the cell lines tested, with 50% growth inhibition (GI_{50}) values in a range of nM - low μ M (Table 1). The pan-CDK inhibitors **9a** ($R^1 = NH_2$, $R^2 = F$, $R^3 = m-SO_2NH_2$) and **9d** ($R^1 = NH_2$, $R^2 = F$, $R^3 = m-4$ -methylpiperazin-1-yl) showed the most potent anti-proliferative properties with GI_{50} values of 0.05 - 0.09 μ M. However a considerable loss in cellular potency was observed with **9n** ($R^1 = NHMe$, $R^2 = CN$, $R^3 = m-CO-4$ -acetyl piperazin-1-yl) giving the GI_{50} values of 4.96 - 5.88 μ M in the tumour cell lines.

3.2. Cellular mechanism of action

Based on the observed CDK9 selectivity and cellular potency, **9s** was selected for detailed cellular mechanistic studies. A panel of cell lines representing a range of tumour types,

including colorectal, breast, lung, ovarian, cervical and pancreatic cancers, were treated with **9s** for 48 h. As shown in Table 2, **9s** exhibited a broad spectrum of anti-proliferative activity with GI_{50} ranging from 0.64 – 2.01 μM . HCT-116 and MCF-7 appeared to be the most sensitive with $GI_{50} = 0.79$ and 0.64 μM respectively. We next investigated whether the anti-proliferative effect of **9s** was a consequence of activation of cellular apoptosis. Induction of caspase 3 activity was measured in HCT-116 cancer cells after treatment with **9s** for 24 h (Figure 2), showing significant activation of caspase 3 at $5\times$ and $10\times$ GI_{50} μM concentrations. Annexin V/PI double staining was then performed to confirm the ability of **9s** in induction of apoptosis. As shown in Figure 3, **9s** effectively induced cell apoptosis (Annexin V positive/PI negative cells) starting from $5\times$ GI_{50} μM with an enhanced effect at higher concentrations. We further examined the effects of a 24-hour exposure of **9s** on cell cycle progression (Figure 4). Flow cytometric analysis of HCT-116 cells indicated a slight increase in G1-phase DNA content at the GI_{50} concentration, but G2-M arrest predominates following drug exposure at higher concentrations ($5\times$ and $10\times$ GI_{50} μM), accompanied by substantial sub-G1 DNA at $10\times$ GI_{50} , indicating cell death. The cell-cycle profile is consistent with that previously observed for other CDK9 inhibitors [20].

Consistent with cellular inhibition of CDK9 by **9s**, western blotting analysis of HCT-116 cells upon 24-hours drug treatment showed that phosphorylation at Ser2 of RNAPII CTD was reduced at 1.0 μM and completely abolished at 5.0 μM (Figure 5). A decrease in phospho-Ser5 as well as total RNA polymerase II levels at 10 μM was also observed. Anti-apoptotic protein Mcl-1 expression was reduced at 1.0 μM , the concentration causing cellular CDK9 inhibition, and completely inhibited at 5.0 μM . This was accompanied by PARP cleavage indicating cell apoptosis.

4. Conclusion

In conclusion, a series of 2,4,5-trisubstituted pyrimidines were synthesized and their structure activity relationship was investigated. Most compounds demonstrated low-nM CDK9 inhibition and anti-proliferative activity in tumour cell lines. Lead compound **9s** showed >20-fold selectivity for CDK9 over CDK1 and CDK2, and 10-fold selectivity over CDK7. The Cellular mode of action investigation confirmed that **9s** is capable of inducing apoptosis through CDK9 mediated down-regulation of anti-apoptotic protein Mcl-1 and activation of caspase-3.

5. Experimental section

5.1. Chemistry

Chemical reagents and solvents were obtained from commercial sources. When necessary, solvents were dried and/or purified by standard methods. ^1H NMR and ^{13}C NMR spectra were obtained using a Bruker 400 Ultrashield spectrometer at 400 and 100 MHz, respectively. These were analyzed using the Bruker TOPSPIN 2.1 program. Chemical shifts are reported in parts per million relative to the residual solvent signal. Coupling constants (J) are quoted to the nearest 0.1 Hz. The following abbreviations are used: s, singlet; d, doublet; t, triplet; q, quartet; m, multiplet; br, broad. High resolution mass spectra were obtained using a Waters 2795 single quadrupole mass spectrometer/micromass LCT platform. Purity for final compounds was greater than 95% and was measured using Waters high performance liquid chromatography (Waters 2487 dual λ absorbance detector) with Phenomenex Gemini-NX 5u C18 110A 250 mm \times 4.60 mm column, UV detector at 254 nm, using system A (10% MeCN containing 0.1% TFA for 2 min, followed by linear gradient 10–100% over 10 min at a flow rate of 1 mL/min); system B (10-70 % MeCN over 20 min at a flow rate of 1 mL/min);

system C (10% MeOH containing 0.1% TFA for 4 min, followed by linear gradient 10–100% over 10 min at a flow rate of 1 mL/min); and system D (10% MeOH containing 0.1% TFA for 4 min, followed by linear gradient 10–100% over 6 min at a flow rate of 1 mL/min). Flash chromatography was performed using either a glass column packed with silica gel (200–400 mesh, Aldrich Chemical) or prepacked silica gel cartridges (FlashMaster systems, Biotage). Melting points were determined with an Electrothermal melting point apparatus and are uncorrected.

5.1.1. N'-(5-(3-(dimethylamino)-2-fluoroacryloyl)-4-methylthiazol-2-yl)-N,N-dimethylformimidamide (4b).

To a well-stirred solution of *N'-(5-(3-(dimethylamino)acryloyl)-4-methylthiazol-2-yl)-N,N*-dimethylformimidamide **3b** (5.0 mmol) in MeOH under ice bath, selectfluor (7.5 mmol) was added and the mixture was stirred for 1 hour. After completion of the reaction, the mixture was concentrated and purified by column chromatography using EtoAc/MeOH to yield the titled compound. Yellow solid (22 %). ¹H-NMR (DMSO-*d*₆): δ 2.41 (s, 3H, CH₃), 2.98 (s, 3H, CH₃), 3.06 (d, 6H, *J* = 1.6 Hz, 2×CH₃), 3.18 (s, 3H, CH₃), 6.95 (d, 1H, *J* = 29.6 Hz, CH), 8.38 (s, 1H, NH). HR-MS (ESI⁺): *m/z* [M + H]⁺ C₁₂H₁₇FN₄OS calcd for 285.1185; found 285.1206.

5.1.2. General method for the synthesis of compounds (9a-9s).

A mixture of the appropriate enaminones **4a-c**, 1-phenylguanidine **8** (2 equivalent mmol) in 2-methoxyethanol (0.2 mL/mmol) was heated in a Discovery Microwave at 100-140 °C for 30-45 minutes. Upon cooling, the residue was purified by flash chromatography using

appropriate mixtures of EtOAc/PE or EtOAc/MeOH as the eluant. The products were further purified by crystallization from EtOAc-MeOH mixtures.

5.1.3. 3-((4-(2-Amino-4-methylthiazol-5-yl)-5-fluoropyrimidin-2-yl)amino)benzenesulfonamide (**9a**).

From *N'*-(5-(3-(dimethylamino)-2-fluoroacryloyl)-4-methylthiazol-2-yl)-*N,N*-dimethylformimidamide and 3-guanidinobenzenesulfonamide. Light Yellow powder (10 %); mp: 264 °C (dec). Anal. RP-HPLC: t_R 9.00 min (method A), purity 95 %. $^1\text{H-NMR}$ (DMSO- d_6): δ 2.48 (d, 3H, $J = 2.0$ Hz, CH_3), 7.30 (s, 2H, NH_2), 7.41 (dt, 1H, $J = 8.0, 1.2$ Hz, Ph-H), 7.47 (t, 1H, $J = 8.0$ Hz, Ph-H), 7.60 (s, 2H, NH_2), 7.91-7.97 (m, 1H, Ph-H), 8.20 (t, 1H, $J = 2.0$ Hz, Ph-H), 8.46 (d, 1H, $J = 3.6$ Hz, Py-H), 9.82 (s, 1H, NH). $^{13}\text{C-NMR}$ (DMSO- d_6): δ 19.19, 109.90 (d, $J = 9.0$ Hz), 115.92, 118.79, 121.90, 129.52, 141.47, 144.91, 145.88 (d, $J = 26$ Hz), 147.82, 147.98 (d, $J = 249$ Hz), 155.47, 156.06, 170.74 (d, $J = 5.0$ Hz). HR-MS (ESI $^+$): m/z $[\text{M} + \text{H}]^+$ calcd for $\text{C}_{14}\text{H}_{14}\text{FN}_6\text{O}_2\text{S}_2$, 381.0604; found 381.0475.

5.1.4. 1-(4-(3-(4-(2-Amino-4-methylthiazol-5-yl)-5-fluoropyrimidin-2-ylamino)phenyl)piperazin-1-yl)ethanone (**9b**).

From 1-(4-acetylpiperazin-1-yl)phenylguanidine and *N'*-(5-(3-(dimethylamino)-2-fluoroacryloyl)-4-methyl thiazol-2-yl)-*N,N*-dimethyl formimidamide. Light Yellow powder (10%); mp 235 °C (dec). Anal. RP-HPLC: t_R 8.90 min (method A), purity 98 %. $^1\text{H-NMR}$ (DMSO- d_6): δ 2.05 (s, 3H, CH_3), 2.41 (d, 3H, $J = 2.8$ Hz, CH_3), 3.08 (apparent t, 2H, $J = 5.2$ Hz, CH_2), 3.15 (apparent t, 2H, $J = 5.2$ Hz, CH_2), 3.53-3.63 (m, 4H, $2 \times \text{CH}_2$), 6.57 (dd, 1H, $J = 8.0, 2.0$ Hz, Ph-H), 7.12 (t, 1H, $J = 8.0$ Hz, Ph-H), 7.22 (dd, 1H, $J = 8.0, 1.2$ Hz, Ph-H), 7.38 (t, 1H, $J = 2.0$ Hz, Ph-H), 7.56 (s, 2H, NH_2), 8.42 (d, 1H, $J = 3.6$ Hz, Py-H), 9.36 (s, 1H,

NH). ^{13}C -NMR (DMSO- d_6): δ 18.98 (d, $J = 6$ Hz), 21.68, 41.17, 45.94, 49.04, 49.47, 107.01, 109.87, 110.80, 110.91 (d, $J = 8$ Hz), 129.31, 141.76, 146.23 (d, $J = 25$ Hz), 147.28 (d, $J = 12$ Hz), 147.71 (d, $J = 248$ Hz), 151.70, 154.26, 156.46 (d, $J = 2$ Hz), 168.78, 170.49 (d, $J = 4$ Hz). HR-MS (ESI+): m/z $[\text{M} + \text{H}]^+$ calcd for $\text{C}_{20}\text{H}_{23}\text{FN}_7\text{OS}$, 428.1669; found 428.1736.

5.1.5 5-(5-Fluoro-2-(3-(4-methylpiperazin-1-yl)phenylamino)pyrimidin-4-yl)-N,4-dimethylthiazol-2-amine (9c).

From 1-(3-(4-methylpiperazin-1-yl)phenyl)guanidine and 3-(dimethylamino)-2-fluoro-1-(4-methyl-2-(methylamino)thiazol-5-yl)prop-2-en-1-one. Yellow solid (10 %); mp 179-180 °C. Anal. RP-HPLC: t_{R} 8.73 min (method A), purity 99 %. ^1H -NMR (DMSO- d_6): δ 2.23 (s, 3H, CH_3), 2.44 (s, 3H, CH_3), 2.80-2.93 (m, 4H, $2\times\text{CH}_2$), 3.12 (s, 4H, $2\times\text{CH}_2$), 6.54 (d, 2H, $J = 6.8$ Hz, Ph-H), 7.09 (t, 1H, $J = 7.6$ Hz, Ph-H), 7.18 (d, 1H, $J = 7.6$ Hz, Ph-H), 7.33 (s, 1H, Ph-H), 8.10 (s, 1H, NH), 8.43 (s, 1H, Py-H), 9.32 (s, 1H, NH). HR-MS (ESI+): m/z $[\text{M} + \text{H}]^+$ calcd for $\text{C}_{20}\text{H}_{25}\text{FN}_7\text{S}$, 414.1876; found 414.1973.

5.1.6 5-(5-Fluoro-2-(3-(4-methylpiperazin-1-yl)phenylamino)pyrimidin-4-yl)-4-methylthiazol-2-amine (9d).

From 1-(3-(4-methylpiperazin-1-yl)phenyl)guanidine and N' -(5-(3-(dimethylamino)-2-fluoroacryloyl)-4-methylthiazol-2-yl)- N,N -dimethylformimidamide. Light yellow powder (6 %); mp 146-148 °C. Anal. RP-HPLC: t_{R} 11.10 min (method C), purity 98 %. ^1H -NMR (DMSO- d_6): δ 2.23 (s, 3H, CH_3), 2.41 (d, 3H, $J = 2.8$ Hz, CH_3), 2.46 (apparent t, 4H, $J = 4.8$ Hz, $2\times\text{CH}_2$), 3.12 (apparent t, 4H, $J = 4.4$ Hz, $2\times\text{CH}_2$), 6.54 (dd, 2H, $J = 8.4, 2.0$ Hz, Ph-H), 7.09 (t, 1H, $J = 8.0$ Hz, Ph-H), 7.18 (d, 1H, $J = 8.0$ Hz, Ph-H), 7.32 (s, 1H, Ph-H), 7.55 (s, 2H,

NH₂), 8.42 (d, 1H, *J* = 3.6 Hz, Py-H), 9.31 (s, 1H, NH). HR-MS (ESI⁺): *m/z* [M + H]⁺ calcd for C₁₉H₂₃FN₇S, 400.1720; found 400.1459.

5.1.7 4-(4-Methyl-2-(methylamino)thiazol-5-yl)-2-((3-(methylsulfonyl)phenyl)amino)pyrimidine-5-carbonitrile (**9e**).

From *tert*-butyl (5-(2-cyano-3-(dimethylamino)acryloyl)-4-methylthiazol-2-yl)(methyl)carbamate and 1-(3-(methylsulfonyl)phenyl)guanidine. Yellow solid (12 %); mp 277-278 °C. Anal. RP-HPLC: *t_R* 5.47 min (method B), purity 97%. ¹H-NMR (DMSO-*d*₆): δ 2.44 (s, 3H, CH₃), 2.90 (d, 3H, *J* = 4.8 Hz, CH₃), 3.21 (s, 3H, CH₃), 7.56-7.66 (m, 2H, 2×Ph-H), 7.93-8.04 (m, 1H, Ph-H), 8.31 (q, 1H, *J* = 4.8 Hz, NH), 8.41 (s, 1H, Ph-H), 8.85 (s, 1H, Py-H), 10.58 (s, 1H, NH). ¹³C-NMR (DMSO-*d*₆): δ 20.08, 31.42, 44.15, 94.78, 118.08, 118.36, 121.59, 125.25, 130.28, 140.39, 141.76, 156.49, 159.20, 161.45, 164.19. HR-MS (ESI⁺): *m/z* [M + H]⁺ calcd for C₁₇H₁₇N₆O₂S₂, 401.0854; found 401.2841.

5.1.8 3-((5-Cyano-4-(4-methyl-2-(methylamino)thiazol-5-yl)pyrimidin-2-yl)amino)-*N*-(2-methoxyethyl)benzenesulfonamide (**9f**).

From *tert*-butyl (5-(2-cyano-3-(dimethylamino)acryloyl)-4-methylthiazol-2-yl)(methyl)carbamate and 3-guanidino-*N*-(2-methoxyethyl)benzenesulfonamide. Yellow solid (7 %); mp 202-203 °C. Anal. RP-HPLC: *t_R* 4.87 min (method B), purity 97 %. ¹H-NMR (DMSO-*d*₆): δ 2.44 (s, 3H, CH₃), 2.89 (d, 3H, *J* = 4.8 Hz, CH₃), 2.93 (q, 2H, *J* = 5.6 Hz, CH₂), 3.16 (s, 3H, CH₃), 3.29 (t, 2H, *J* = 5.6 Hz, CH₂), 7.48 (dt, 1H, *J* = 8.0, 1.6 Hz, Ph-H), 7.56 (t, 1H, *J* = 8.0 Hz, Ph-H), 7.71 (t, 1H, *J* = 5.6 Hz, NH), 7.93 (d, 1H, *J* = 8.4 Hz, Ph-H), 8.24 (s, 1H, Ph-H), 8.29 (q, 1H, *J* = 4.8 Hz, NH), 8.83 (s, 1H, Py-H), 10.50 (br s, 1H, NH). ¹³C-NMR (DMSO-*d*₆): δ 20.03, 31.39, 42.67, 58.31, 70.97, 94.65, 118.12, 118.48,

121.16, 124.20, 129.95, 140.06, 141.65, 159.27, 161.48, 164.16, 170.91. HR-MS (ESI+): m/z [M + H]⁺ calcd for C₁₉H₂₂N₇O₃S₂, 460.1226; found, 460.1713.

5.1.9 3-(5-Fluoro-4-(4-methyl-2-(methylamino)thiazol-5-yl)pyrimidin-2-ylamino)-N-(2-methoxyethyl)benzenesulfonamide (**9g**).

From 3-guanidino-N-(2-methoxyethyl)benzenesulfonamide and 1-(4-(4-(5-fluoro-4-(4-methyl-2-(methylamino)thiazol-5-yl)pyrimidin-2-ylamino)phenyl)piperazin-1-yl)ethanone.

Yellow solid (20 %); mp: 193-195 °C. Anal. RP-HPLC: t_R 13.97 min (method C), purity 100 %. ¹H-NMR (DMSO-*d*₆): δ 2.49 (s, 3H, CH₃), 2.88 (d, 3H, J = 4.8 Hz, CH₃), 2.93 (q, 2H, J = 6.0 Hz, CH₂), 3.16 (s, 3H, CH₃), 3.31 (t, 2H, J = 6.0 Hz, CH₂), 7.36 (dt, 1H, J = 8.0, 1.6 Hz, Ph-H), 7.49 (t, 1H, J = 8.0 Hz, Ph-H), 7.65 (t, 1H, J = 5.6 Hz, NH), 7.92 (dd, 1H, J = 8.4, 1.6 Hz, Ph-H), 8.14 (q, 1H, J = 4.8 Hz, NH), 8.23 (t, 1H, J = 2.0 Hz, Ph-H), 8.47 (d, 1H, J = 3.6 Hz, Py-H), 9.85 (s, 1H, NH). ¹³C-NMR (DMSO-*d*₆): δ 19.38 (d, J = 5 Hz), 31.34, 42.65, 58.32, 70.99, 110.05 (d, J = 8 Hz), 116.57, 119.29, 122.30, 129.75, 141.46, 141.67, 145.99 (d, J = 25 Hz), 147.62 (d, J = 12 Hz), 147.98 (d, J = 249 Hz), 155.59, 155.99, 171.36. HR-MS (ESI+): m/z [M + H]⁺ calcd for C₁₈H₂₂FN₆O₃S₂, 453.1179; found 453.0728.

5.1.10 4-(4-Methyl-2-(methylamino)thiazol-5-yl)-2-((3 (morpholinosulfonyl)phenyl)amino)pyrimidine-5-carbonitrile (**9h**).

From *tert*-butyl (5-(2-cyano-3-(dimethylamino)acryloyl)-4-methylthiazol-2-yl)(methyl)carbamate and 1-(3-(morpholinosulfonyl)-phenyl)guanidine. Yellow solid (25 %); mp: 240-241 °C. Anal. RP-HPLC: t_R 9.8 min (method B), purity 95 %. ¹H-NMR (DMSO-*d*₆): δ 2.43 (s, 3H, CH₃), 2.89 (d, 7H, J = 4.8 Hz, CH₃ & 2 × CH₂), 3.63 (apparent t, 4H, J = 4.8 Hz, 2×CH₂), 7.40 (d, 1H, J = 8.4 Hz, Ph-H), 7.63 (t, 1H, J = 8.0 Hz, Ph-H), 8.03 (d, 1H,

$J = 8.0$ Hz, Ph-H), 8.22 (s, 1H, Ph-H), 8.29 (q, 1H, $J = 4.8$ Hz, NH), 8.85 (s, 1H, Py-H), 10.55 (br s, 1H, NH). $^{13}\text{C-NMR}$ (DMSO- d_6): δ 19.98, 31.38, 46.41, 65.74, 95.03, 118.03, 119.08, 122.21, 125.04, 130.19, 135.38, 140.48, 159.24, 161.57, 164.15, 170.93. HR-MS (ESI+): m/z [M + H] $^+$ calcd for $\text{C}_{20}\text{H}_{22}\text{N}_7\text{O}_3\text{S}_2$, 472.1226; found, 472.1476.

5.1.11 5-(5-Fluoro-2-(4-methyl-3-(morpholinosulfonyl)phenylamino)pyrimidin-4-yl)-N,4-dimethylthiazol-2-amine (**9j**).

From 1-(4-methyl-3-(morpholinosulfonyl) phenyl)guanidine and 1-(4-(4-(5-fluoro-4-(4-methyl-2-(methylamino)thiazol-5-yl)pyrimidin-2-ylamino)phenyl)piperazin-1-yl)ethanone. Yellow solid (19 %); mp: 232-234 °C. Anal. RP-HPLC: t_R 14.75 min (method A), purity 100 %. $^1\text{H-NMR}$ (DMSO- d_6): δ 2.48 (d, 3H, $J = 2.8$ Hz, CH_3), 2.88 (d, 3H, $J = 4.8$ Hz, CH_3), 3.05 (apparent t, 4H, $J = 4.8$ Hz, $2 \times \text{CH}_2$), 3.63 (apparent t, 4H, $J = 4.8$ Hz, $2 \times \text{CH}_2$), 7.36 (d, 1H, $J = 4.8$ Hz, Ph-H), 7.95 (dd, 1H, $J = 8.4, 2.4$ Hz, Ph-H), 8.13 (q, 1H, $J = 4.8$ Hz, NH), 8.16 (d, 1H, $J = 2.4$ Hz, Ph-H), 8.46 (d, 1H, $J = 3.2$ Hz, Py-H), 9.78 (s, 1H, NH). $^{13}\text{C-NMR}$ (DMSO- d_6): δ 19.34 (d, $J = 5$ Hz), 20.12, 31.32, 45.77, 60.22, 66.04, 110.06 (d, $J = 8$ Hz), 119.66, 123.17, 129.66, 133.51, 135.04, 139.44, 145.95 (d, $J = 27$ Hz), 147.70 (d, $J = 13$ Hz), 147.26 (d, $J = 248$ Hz), 155.37, 156.04, 171.24. HR-MS (ESI+): m/z [M + H] $^+$ calcd for $\text{C}_{20}\text{H}_{24}\text{FN}_6\text{O}_3\text{S}_2$, 479.1335; found 479.1472.

5.1.12 4-(4-Methyl-2-(methylamino)thiazol-5-yl)-2-((3-((4-methylpiperazin-1-yl)sulfonyl)phenyl)amino)pyrimidine-5-carbonitrile (**9k**).

From *tert*-butyl (5-(2-cyano-3-(dimethylamino)acryloyl)-4-methylthiazol-2-yl)(methyl)carbamate and 1-(3-((4-methylpiperazin-1-yl)sulfonyl)phenyl)guanidine. Brown solid (17 %); mp: > 300 °C. Anal. RP-HPLC: t_R 11.03 min (method D), purity 97 %. $^1\text{H-NMR}$

NMR (DMSO- d_6): δ 2.12 (br s, 3H, CH₃), 2.30-2.38 (m, 2H, CH₂), 2.40-2.46 (m, 2H, CH₂), 2.84-2.95 (m, 7H, CH₃ & 2 \times CH₂), 3.33 (s, 3H, CH₃), 7.39 (d, 1H, J = 7.9 Hz, Ph-H), 7.60 (t, 1H, J = 8.0 Hz, Ph-H), 8.01 (d, 1H, J = 7.9 Hz, Ph-H), 8.21 (br s, 1H, Ph-H), 8.30 (q, 1H, J = 4.8 Hz, NH), 8.84 (s, 1H, Py-H), 10.54 (br s, 1H, NH). ¹³C-NMR (DMSO- d_6): δ 19.5, 30.9, 45.3, 45.8, 53.5, 94.5, 114.1, 117.6, 118.5, 121.6, 124.4, 129.6, 135.4, 139.9, 155.8, 158.8, 161.1, 163.7, 170.6. HR-MS (ESI+): m/z [M + H]⁺ calcd for C₂₁H₂₅N₈O₂S₂ 485.1536; found, 485.1530.

5.1.13 (3-((4-(4-Methyl-2-(methylamino)thiazol-5-yl)pyrimidin-2-yl)amino)phenyl)
(morpholino)methanone (**9l**).

From 3-(dimethylamino)-1-(4-methyl-2-(methylamino)thiazol-5-yl)prop-2-en-1-one and 1-(3-(morpholine-4-carbonyl)phenyl)guanidine. Yellow solid (64 %); mp 262-264 °C. Anal. RP-HPLC: t_R 11.56 min (method B), purity 100 %. ¹H-NMR (DMSO- d_6): δ 2.48 (s, 3H, CH₃), 2.86 (d, 3H, J = 4.8 Hz, CH₃), 3.61 (s, 8H, 4 \times CH₂), 6.90-7.00 (m, 2H, Py-H & Ph-H), 7.35 (t, 1H, J = 8.0 Hz, Ph-H), 7.81 (dd, 1H, J = 8.4, 1.2 Hz, Ph-H), 7.90 (s, 1H, CH), 8.08 (q, 1H, J = 4.8 Hz, NH), 8.35 (d, 1H, J = 5.2 Hz, Py-H), 9.60 (s, 1H, NH). ¹³C-NMR (DMSO- d_6): δ 19.11, 31.33, 66.62, 107.64, 117.45, 118.17, 119.97, 120.04, 129.03, 136.25, 141.17, 153.06, 158.09, 159.11, 159.81, 169.73, 169.94. HR-MS (ESI+): m/z [M + H]⁺ calcd for C₂₀H₂₃N₆O₂S, 411.1603; found, 411.1607.

5.1.14 2-((3-(4-Acetylpiperazine-1-carbonyl)phenyl)amino)-4-(4-methyl-2-(methylamino)thiazol-5-yl)pyrimidine-5-carbonitrile (**9n**).

From *tert*-butyl (5-(2-cyano-3-(dimethylamino)acryloyl)-4-methylthiazol-2-yl)(methyl)carbamate and carbonylacrylonitrile and 1-(3-(4-acetylpiperazine-1-

carbonyl)phenyl)guanidine. Yellow solid (54 %); mp 200-201°C. Anal. RP-HPLC: t_R 8.12 min (method B), purity 100 %. 1H -NMR (DMSO- d_6): δ 2.02 (s, 3H, CH₃), 2.42 (s, 3H, CH₃), 2.88 (d, 3H, J = 4.8 Hz, CH₃), 3.45 (br s, 8H, 4×CH₂), 7.11 (d, 1H, J = 7.6 Hz Ph-H), 7.42 (t, 1H, J = 8.0 Hz Ph-H), 7.75 (d, 1H, J = 8.0 Hz Ph-H), 7.90 (s, 1H, Ph-H), 8.26 (q, 1H, J = 4.8 Hz, NH), 8.81 (s, 1H, Py-H), 10.39 (br s, 1H, NH). ^{13}C -NMR (DMSO- d_6): δ 19.89, 21.69, 31.31, 94.50, 118.15, 119.20, 121.88, 122.03, 129.29, 136.42, 139.51, 159.36, 161.51, 164.05, 169.00, 169.50, 170.65. HR-MS (ESI+): m/z [M + H]⁺ calcd for C₂₃H₂₅N₈O₂S, 477.1821; found, 477.1925.

5.1.15 4-(4-Methyl-2-(methylamino)thiazol-5-yl)-2-((3-(4-methylpiperazine-1-carbonyl)phenyl)amino)pyrimidine-5-carbonitrile (**9o**).

From *tert*-butyl (5-(2-cyano-3-(dimethylamino)acryloyl)-4-methylthiazol-2-yl)(methyl)carbamate and 1-(3-(4-methylpiperazine-1-carbonyl)phenyl)guanidine. Yellow solid (21 %); mp 139-140 °C. Anal. RP-HPLC: t_R 3.04 min (method B), purity 100 %. 1H -NMR (MEOD- d_4): δ 0.80 (s, 3H, CH₃), 0.89 (s, 2H, CH₂), 0.97 (s, 3H, CH₃), 1.03 (s, 2H, CH₂), 1.48 (s, 3H, CH₃), 2.00 (s, 2H, CH₂), 2.28 (s, 2H, CH₂), 5.71 (d, 1H, J = 7.6 Hz, Ph-H), 5.92 (t, 1H, J = 7.6 Hz, Ph-H), 6.17 (d, 1H, J = 7.6 Hz, Ph-H), 6.52 (s, 1H, Ph-H), 7.17 (s, 1H, Py-H). ^{13}C -NMR (DMSO- d_6): δ 19.92, 31.35, 45.99, 54.69, 94.47, 118.16, 118.98, 121.62, 121.89, 129.25, 136.74, 139.46, 159.34, 161.51, 164.02, 169.22. HR-MS (ESI+): m/z [M + H]⁺ calcd for C₂₂H₂₅N₈OS, 449.1827; found, 449.3006.

5.1.16 2-((2-Chloro-5-(4-methylpiperazine-1-carbonyl)phenyl)amino)-4-(4-methyl-2-(methylamino)thiazol-5-yl)pyrimidine-5-carbonitrile (**9p**).

From *tert*-butyl (5-(2-cyano-3-(dimethylamino)acryloyl)-4-methylthiazol-2-yl)(methyl)carbamate and 1-(2-chloro-5-(4-methylpiperazine-1-carbonyl)phenyl)guanidine. Yellow solid (9 %); mp: 162-163 °C. Anal. RP-HPLC: t_R 3.04 min (method B), purity 100 %. $^1\text{H-NMR}$ (MEOD- d_4): δ 0.89 (s, 3H, CH₃), 0.97 (s, 3H, CH₃), 1.18 (br s, 4H, 2×CH₂), 1.47 (s, 3H, CH₃), 2.15 (br s, 4H, 2×CH₂), 5.77 (dd, 1H, $J = 8.0, 2.0$ Hz, Ph-H), 6.11 (apparent d, 1H, $J = 8.0$ Hz, Ph-H), 6.60 (d, 1H, $J = 1.6$ Hz, Ph-H), 7.16 (s, 1H, Py-H). HR-MS (ESI⁺): m/z [M + H]⁺ calcd for C₂₂H₂₄ClN₈OS, 483.1482; find 483.1646.

5.1.17 3-(5-Fluoro-4-(4-methyl-2-(methylamino)thiazol-5-yl)pyrimidin-2-ylamino)-N-(1-methylpiperidin-4-yl)benzamide (**9q**).

From 3-guanidino-N-(1-methylpiperidin-4-yl)benzamide and (5-(3-(dimethylamino)-2-fluoroacryloyl)-4-methyl thiazol-2-yl)-N,N-dimethyl formimidamide. Yellow solid (10 %); mp: 235-237 °C. Anal. RP-HPLC: t_R 8.60 min (method A), purity 100 %. $^1\text{H-NMR}$ (DMSO- d_6): δ 1.51-1.66 (m, 2H, CH₂), 1.76 (apparent d, 2H, $J = 10.4$ Hz, CH₂), 1.99 (t, 2H, $J = 12.0$ Hz, CH₂), 2.19 (s, 3H, CH₃), 2.48 (d, 3H, $J = 1.6$ Hz, CH₃), 2.79 (d, 2H, $J = 11.2$ Hz, CH₂), 2.88 (d, 3H, $J = 4.8$ Hz, CH₃), 3.67-3.80 (m, 1H, CH), 7.30-7.34 (m, 2H, 2×Ph-H), 7.80 (d, 1H, $J = 8.0$ Hz, Ph-H), 8.07-8.21 (m, 3H, Ph-H & 2×NH), 8.44 (d, 1H, $J = 3.2$ Hz, Py-H), 9.62 (s, 1H, NH). $^{13}\text{C-NMR}$ (DMSO- d_6): δ 19.41, 31.29, 31.72, 46.24, 46.80, 54.85, 109.99, 118.72, 120.47, 121.72, 128.57, 135.92, 140.98, 146.06 (d, $J = 26$ Hz), 147.41 (d, $J = 12$ Hz), 147.78 (d, $J = 248$ Hz), 155.42, 156.29, 166.58, 171.13. HR-MS (ESI⁺): m/z [M + H]⁺ calcd for C₂₂H₂₇FN₇OS, 456.1982; found 456.1998.

5.1.18 4-(5-Cyano-4-(4-methyl-2-(methylamino)thiazol-5-yl)pyrimidin-2-ylamino)-N-(1-methylpiperidin-4-yl)benzamide (**9r**).

From 4-guanidino-*N*-(1-methylpiperidin-4-yl)benzamide and 3-(dimethylamino)-2-(4-methyl-2-(methylamino)thiazole-5-carbonyl)acrylonitrile. Yellow solid (13 %); mp: 230-232 °C. Anal. RP-HPLC: t_R 8.40 min (method A), purity 100 %. $^1\text{H-NMR}$ (DMSO- d_6): δ 1.52-1.66 (m, 2H, CH₂), 1.76 (apparent d, 2H, $J = 9.6$ Hz, CH₂), 2.00 (t, 2H, $J = 10.8$ Hz, CH₂), 2.20 (s, 3H, CH₃), 2.44 (s, 3H, CH₃), 2.81 (d, 2H, $J = 11.6$ Hz, CH₂), 2.90 (d, 3H, $J = 4.4$ Hz, CH₃), 3.68-3.80 (m, 1H, CH), 7.78-7.89 (m, 4H, 4×Ph-H), 8.13 (d, 1H, $J = 7.6$ Hz, NH), 8.28 (q, 1H, $J = 4.4$ Hz, NH), 8.83 (s, 1H, Py-H), 10.45 (s, 1H, NH). $^{13}\text{C-NMR}$ (DMSO- d_6): δ 20.02, 31.32, 31.74, 46.19, 46.79, 54.85, 94.66, 114.35, 118.12, 119.66, 128.42, 129.23, 141.99, 155.95, 159.20, 161.47, 164.06, 165.68, 170.75. HR-MS (ESI⁺): m/z [M + H]⁺ calcd for C₂₃H₂₇N₈OS, 463.2029; found 463.1533.

5.1.19 3-(5-Cyano-4-(4-methyl-2-(methylamino)thiazol-5-yl)pyrimidin-2-ylamino)-*N*-(1-methylpiperidin-4-yl)benzamide (**9s**).

From 3-guanidino-*N*-(1-methylpiperidin-4-yl)benzamide and 3-(dimethylamino)-2-(4-methyl-2-(methylamino)thiazole-5-carbonyl)acrylonitrile. Yellow solid (18 %); mp: 168-170 °C. Anal. RP-HPLC: t_R 8.39 min (method A), purity 99 %. $^1\text{H-NMR}$ (DMSO- d_6): δ 1.51-1.63 (m, 2H, CH₂), 1.76 (apparent d, 2H, $J = 10.0$ Hz, CH₂), 1.99 (t, 2H, $J = 11.2$ Hz, CH₂), 2.19 (s, 3H, CH₃), 2.42 (s, 3H, CH₃), 2.79 (d, 2H, $J = 11.2$ Hz, CH₂), 2.89 (d, 3H, $J = 4.8$ Hz, CH₃), 3.17 (s, 3H, CH₃), 3.68-3.80 (m, 1H, CH), 7.40 (t, 1H, $J = 8.0$ Hz, Ph-H), 7.51 (d, 1H, $J = 8.0$ Hz, Ph-H), 7.81 (d, 1H, $J = 7.6$ Hz, Ph-H), 8.17 (s, 1H, Ph-H), 8.21 (d, 1H, $J = 7.6$ Hz, NH), 8.28 (q, 1H, $J = 4.8$ Hz, NH), 8.79 (s, 1H, Py-H), 10.32 (s, 1H, NH). $^{13}\text{C-NMR}$ (DMSO- d_6): δ 20.03, 31.31, 31.70, 46.24, 46.86, 54.83, 93.99, 118.29, 120.53, 122.33, 123.60, 128.77, 135.95, 139.32, 156.49, 159.42, 161.40, 164.11, 166.21, 170.64. HR-MS (ESI⁺): m/z [M + H]⁺ C₂₃H₂₇N₈OS, 463.2027; found 463.2188.

5.2. Modelling Methods

Up to 2000 conformations of the individual compounds to be docked were generated using OpenEye OMEGA software (version 2.4.6), with all other settings on default. Receptors of PDB structures 4BCF, 4BCG and 4BCP were generated using the OpenEye MAKE RECEPTOR program, using default settings. Hydrogen bond acceptor constraints between the ligand and the amide nitrogen of Cys106 (CDK9) or Leu83 (CDK2) and hydrogen bond donor constraints between the ligand and the carbonyl of Cys106 (CDK9) or Leu83 (CDK2) were enforced. Docking was performed using OpenEye OEDOCK software (version 3.0.0). The number of alternate poses returned was set to 10 and all other settings were on default. FRED Chemgauss 4 was used as the scoring function. Results were visualised using OpenEye VIDA software (version 4.1.2) and images generated using DeLano Scientific LLC PyMOL freeware (version 0.99).

5.3. Biological assays

5.3.1 Kinase assay

Inhibition of kinases was measured by radiometric assay using the Millipore KinaseProfiler services. Half-maximal inhibition (IC_{50}) values were calculated from 10-point dose-response curves and apparent inhibition constants (K_i) were calculated from the IC_{50} values and appropriate K_M (ATP) values for the kinases in question.

5.3.2 MTT toxicity assays

All cancer cell lines were obtained from the cell bank at the Centre for Biomolecular Sciences, University of Nottingham, UK, and were maintained in RPMI-1640 with 10% FBS.

MTT (3-(4,5-dimethylthiazol-2-yl)-2,5-diphenyltetrazolium bromide, Sigma) assays were performed as reported previously [27]. The concentrations required to inhibit 50% of cell growth (GI_{50}) were calculated using non-linear regression analysis.

5.3.3 Caspase-3 assay

Caspase-3 activity was determined following the manufacturer's instructions (CASP3F-1KT, Sigma). Fluorescence was measured at 460 nm at room temperature using an EnVision multilabel plate reader (PerkinElmer).

5.3.4 Annexin V/PI staining and Cell cycle analysis

Cells (2×10^5) were seeded in 6-well plate and were treated with varying concentrations of inhibitor for 24 hours. Cell cycle status was analyzed using a Beckman Coulter EPICS-XL MCL flow cytometer, and data were analyzed using EXPO32 software. Apoptosis was also confirmed using FITC annexin V/PI (propidium iodide) staining according to the protocols (BD Bioscience). The annexin V/PI positive apoptotic cells were enumerated using flow cytometry. The percentage of cells undergoing apoptosis was defined as the sum of early apoptosis (annexin V-positive and PI-negative cells) and late apoptosis (annexin V-positive and PI-positive cells).

5.3.5 Western blots

Western blotting was performed either with Simple Western assay by Simon (Protein Simple) according to manufacturer instruction or as previously described. Antibodies used were as follows: total RNAPII, phosphorylated RNAPII Ser2 and Ser5 (Covance), β -Actin, Mcl-1, and PARP (Cell Signalling Technologies). Both anti-mouse and anti-rabbit

immunoglobulin G (IgG) horseradish peroxidase conjugated antibodies were obtained from Dako.

ACKNOWLEDGMENTS

This study was supported by Cancer Research UK Grants C21568/A8988 and C21568/A12474.

References

- [1] S. Lapenna, A. Giordano, Cell cycle kinases as therapeutic targets for cancer, *Nat Rev Drug Discov*, 8 (2009) 547-566.
- [2] G.I. Shapiro, Cyclin-dependent kinase pathways as targets for cancer treatment, *J Clin Oncol*, 24 (2006) 1770-1783.
- [3] M. Malumbres, R. Sotillo, D. Santamaria, J. Galan, A. Cerezo, S. Ortega, P. Dubus, M. Barbacid, Mammalian cells cycle without the D-type cyclin-dependent kinases Cdk4 and Cdk6, *Cell*, 118 (2004) 493-504.
- [4] D. Cai, V.M. Latham, Jr., X. Zhang, G.I. Shapiro, Combined depletion of cell cycle and transcriptional cyclin-dependent kinase activities induces apoptosis in cancer cells, *Cancer research*, 66 (2006) 9270-9280.
- [5] C. Berthet, E. Aleem, V. Coppola, L. Tessarollo, P. Kaldis, Cdk2 knockout mice are viable, *Curr Biol*, 13 (2003) 1775-1785.
- [6] C. Barriere, D. Santamaria, A. Cerqueira, J. Galan, A. Martin, S. Ortega, M. Malumbres, P. Dubus, M. Barbacid, Mice thrive without Cdk4 and Cdk2, *Mol Oncol*, 1 (2007) 72-83.

- [7] D. Santamaria, C. Barriere, A. Cerqueira, S. Hunt, C. Tardy, K. Newton, J.F. Caceres, P. Dubus, M. Malumbres, M. Barbacid, Cdk1 is sufficient to drive the mammalian cell cycle, *Nature*, 448 (2007) 811-U818.
- [8] M. Guha, Blockbuster dreams for Pfizer's CDK inhibitor, *Nat Biotechnol*, 31 (2013) 187-187.
- [9] M. Malumbres, P. Pevarello, M. Barbacid, J.R. Bischoff, CDK inhibitors in cancer therapy: what is next?, *Trends Pharmacol Sci*, 29 (2008) 16-21.
- [10] R.P. Fisher, Secrets of a double agent: CDK7 in cell-cycle control and transcription, *Journal of cell science*, 118 (2005) 5171-5180.
- [11] R. Shiekhatar, F. Mermelstein, R.P. Fisher, R. Drapkin, B. Dynlacht, H.C. Wessling, D.O. Morgan, D. Reinberg, Cdk-Activating Kinase Complex Is a Component of Human Transcription Factor Tfiif, *Nature*, 374 (1995) 283-287.
- [12] D.H. Price, P-TEFb, a cyclin-dependent kinase controlling elongation by RNA polymerase II, *Molecular and cellular biology*, 20 (2000) 2629-2634.
- [13] R.M. Marshall, X. Grana, Mechanisms controlling CDK9 activity, *Front Biosci*, 11 (2006) 2598-2613.
- [14] S. Wang, P.M. Fischer, Cyclin-dependent kinase 9: a key transcriptional regulator and potential drug target in oncology, virology and cardiology, *Trends Pharmacol Sci*, 29 (2008) 302-313.
- [15] R. Chen, M.J. Keating, V. Gandhi, W. Plunkett, Transcription inhibition by flavopiridol: mechanism of chronic lymphocytic leukemia cell death, *Blood*, 106 (2005) 2513-2519.
- [16] L. Meijer, E. Raymond, Roscovitine and other purines as kinase inhibitors. From starfish oocytes to clinical trials, *Accounts Chem Res*, 36 (2003) 417-425.

- [17] S.J. McClue, D. Blake, R. Clarke, A. Cowan, L. Cummings, P.M. Fischer, M. MacKenzie, J. Melville, K. Stewart, S. Wang, N. Zhelev, D. Zheleva, D.P. Lane, In vitro and in vivo antitumor properties of the cyclin dependent kinase inhibitor CYC202 (R-roscovitine), *International journal of cancer. Journal international du cancer*, 102 (2002) 463-468.
- [18] K. Bettayeb, D. Baunbaek, C. Delehouze, N. Loaec, A.J. Hole, S. Baumli, J.A. Endicott, S. Douc-Rasy, J. Benard, N. Oumata, H. Galons, L. Meijer, CDK Inhibitors Roscovitine and CR8 Trigger Mcl-1 Down-Regulation and Apoptotic Cell Death in Neuroblastoma Cells, *Genes & cancer*, 1 (2010) 369-380.
- [19] M. Guha, Cyclin-dependent kinase inhibitors move into Phase III, *Nat Rev Drug Discov*, 11 (2012) 892-894.
- [20] H. Shao, S. Shi, S. Huang, A.J. Hole, A.Y. Abbas, S. Baumli, X. Liu, F. Lam, D.W. Foley, P.M. Fischer, M. Noble, J.A. Endicott, C. Pepper, S. Wang, Substituted 4-(thiazol-5-yl)-2-(phenylamino)pyrimidines are highly active CDK9 inhibitors: synthesis, X-ray crystal structures, structure-activity relationship, and anticancer activities, *Journal of medicinal chemistry*, 56 (2013) 640-659.
- [21] P.M. Lukasik, S. Elabar, F. Lam, H. Shao, X. Liu, A.Y. Abbas, S. Wang, Synthesis and biological evaluation of imidazo[4,5-b]pyridine and 4-heteroaryl-pyrimidine derivatives as anti-cancer agents, *European journal of medicinal chemistry*, 57 (2012) 311-322.
- [22] H.M. Alkahtani, A.Y. Abbas, S. Wang, Synthesis and biological evaluation of benzo[d]imidazole derivatives as potential anti-cancer agents, *Bioorganic & medicinal chemistry letters*, 22 (2012) 1317-1321.
- [23] S.D. Wang, G. Griffiths, C.A. Midgley, A.L. Barnett, M. Cooper, J. Grabarek, L. Ingram, W. Jackson, G. Kontopidis, S.J. McClue, C. McInnes, J. McLachlan, C. Meades, M. Mezna, I. Stuart, M.P. Thomas, D.I. Zheleva, D.P. Lane, R.C. Jackson, D.M. Glover, D.G. Blake, P.M.

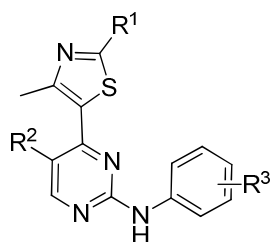
Fischer, Discovery and Characterization of 2-Anilino-4-(Thiazol-5-yl)Pyrimidine Transcriptional CDK Inhibitors as Anticancer Agents, *Chem Biol*, 17 (2010) 1111-1121.

[24] S.D. Wang, C. Meades, G. Wood, A. Osnowski, S. Anderson, R. Yuill, M. Thomas, M. Mezna, W. Jackson, C. Midgley, G. Griffiths, I. Fleming, S. Green, I. McNae, S.Y. Wu, C. McInnes, D. Zheleva, M.D. Walkinshaw, P.M. Fischer, 2-anilino-4-(thiazol-5-yl)pyrimidine CDK inhibitors: Synthesis, SAR analysis, X-ray crystallography, and biological activity, *Journal of medicinal chemistry*, 47 (2004) 1662-1675.

[25] A.J. Hole, S. Baumli, H. Shao, S. Shi, S. Huang, C. Pepper, P.M. Fischer, S. Wang, J.A. Endicott, M.E. Noble, Comparative structural and functional studies of 4-(thiazol-5-yl)-2-(phenylamino)pyrimidine-5-carbonitrile CDK9 inhibitors suggest the basis for isotype selectivity, *Journal of medicinal chemistry*, 56 (2013) 660-670.

[26] G. Nemeth, Z. Varga, Z. Greff, G. Bencze, A. Sipos, C. Szantai-Kis, F. Baska, A. Gyuris, K. Kelemenics, Z. Szathmary, J. Minarovits, G. Keri, L. Orfi, Novel, selective CDK9 inhibitors for the treatment of HIV infection, *Current medicinal chemistry*, 18 (2011) 342-358.

[27] X. Liu, S. Shi, F. Lam, C. Pepper, P.M. Fischer, S. Wang, CDKI-71, a novel CDK9 inhibitor, is preferentially cytotoxic to cancer cells compared to flavopiridol, *International journal of cancer. Journal international du cancer*, 130 (2012) 1216-1226.

Table 1 Structure and biological activity summary

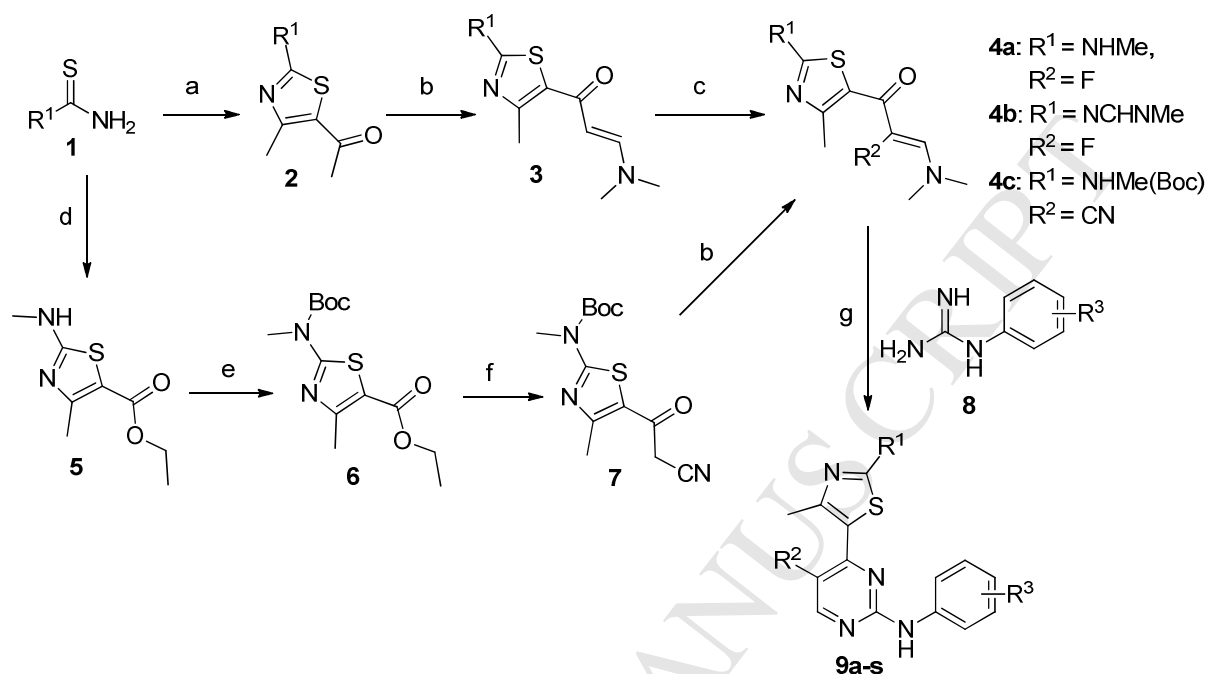
Comp	Structure			Kinase inhibition K_i (nM) ^a				Cytotoxicity (GI_{50} , μ M) ^b	
	R ¹	R ²	R ³	CDK9T1	CDK1B	CDK2A	CDK7H	HCT-116	MCF-7
9a	NH ₂	F	<i>m</i> -SO ₂ NH ₂	3	7	3	252	0.05	0.41
9b	NH ₂	F	<i>m</i> -4-acetylpiperazin-1-yl	11	41	77	1,457	0.17	0.42
9c	NHMe	F	<i>m</i> -4-methylpiperazin-1-yl	7	32	41	541	0.51	0.62
9d	NH ₂	F	<i>m</i> -4-methylpiperazin-1-yl	11	65	68	476	0.09	0.09
9e	NHMe	CN	<i>m</i> -SO ₂ Me	5	19	43	110	0.20	0.43
9f	NHMe	CN	<i>m</i> -SO ₂ NH(CH ₂) ₂ OCH ₃	16	34	22	180	0.19	0.26
9g	NHMe	F	<i>m</i> -SO ₂ NH(CH ₂) ₂ OCH ₃	3	10	6	30	0.30	0.72
9h	NHMe	CN	<i>m</i> -SO ₂ -morpholine	14	73	55	893	0.30	0.82
9i	NHMe	H	<i>m</i> -SO ₂ -morpholine, <i>p</i> -Me	27	357	294	150	0.94	1.61
9j	NHMe	F	<i>m</i> -SO ₂ -morpholine, <i>p</i> -Me	11	101	130	133	0.70	1.50
9k	NHMe	CN	<i>m</i> -SO ₂ -4-methylpiperazin-1-yl	35	576	584	24	0.61	1.15
9l	NHMe	H	<i>m</i> -CO-morpholine	95	261	485	393	0.52	0.55
9m	NHMe	CN	<i>m</i> -CO-morpholine	43	205	199	1,870	0.59	0.82
9n	NHMe	CN	<i>m</i> -CO-4-acetylpiperazin-1-yl	17	166	134	552	5.88	4.96
9o	NHMe	CN	<i>m</i> -CO-4-methylpiperazin-1-yl	19	313	164	840	0.72	1.38
9p	NHMe	CN	<i>m</i> -CO-4-methylpiperazin-1-yl, <i>o</i> -Cl	715	>5,000	>5,000	>5,000	1.47	1.93
9q	NHMe	F	<i>m</i> -CO- <i>N</i> -(1-methylpiperidin-4-yl)	36	64	231	542	0.47	0.94
9r	NHMe	CN	<i>p</i> -CO- <i>N</i> -(1-methylpiperidin-4-yl)	8	43	32	304	0.18	0.51
9s	NHMe	CN	<i>m</i> -CO- <i>N</i> -(1-methylpiperidin-4-yl)	14	262	316	163	0.79	0.64

^aApparent inhibition constants (K_i) were calculated from IC₅₀ values and the appropriate K_m

(ATP) values for each kinase. ^bAnti-proliferative activity by MTT-48 h assay; the data given are mean values derived from at least three replicates.

Table 2 Anti-proliferative activity of **9s** in human cancer cell lines

Human Cell line		48h-MTT
Origin	Designation	GI ₅₀ (μM) ± S.D.
Colon Carcinoma	HCT-116	0.79 ± 0.08
Breast Carcinoma	MCF-7	0.64 ± 0.08
	MDA-MB468	1.51 ± 0.34
Lung Carcinoma	A549	2.01 ± 0.55
Ovarian Carcinoma	A2780	1.00 ± 0.11
Cervical Carcinoma	HeLa	0.90 ± 0.07
Pancreatic carcinoma	Miacapa-2	1.25 ± 0.26



Scheme 1 Synthesis of 2,4,5-trisubstituted pyrimidines. Reagents and conditions: (a) 3-Chloro-2,4-pentadione, MeOH, pyridine, r.t., 4 h; (b) *N,N*-dimethylformamide dimethyl acetal (DMF-DMA), Δ , overnight or MeCN, discovery microwave, 140 °C, 45 min.; (c) Selectfluor, MeOH, 0 °C, 1 h; (d) Ethyl 2-chloro-3-oxobutanoate, MeOH, pyridine, r.t., 4 h; (e) Di-*tert*-butyl dicarbonate, 4-dimethylaminopyridine (DMAP), DCM, r.t., 1 h; (f) Lithium diisopropyl amide (LDA), MeCN, THF, -78 °C, 1.5 h; (g) 2-Methoxyethanol, discovery microwave, 140 °C, 20-45 min.

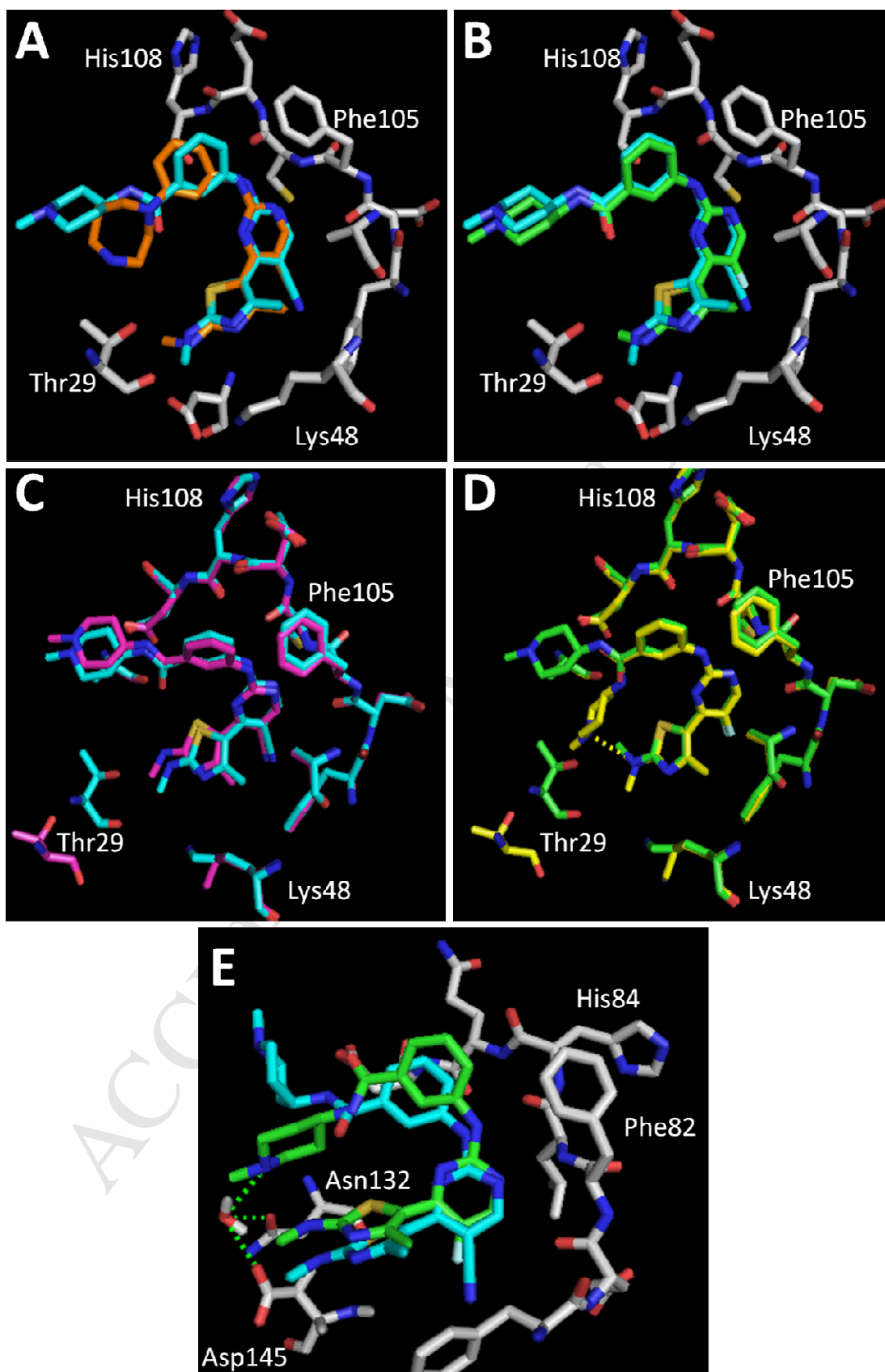


Figure 1 Rational for selectivity: **A.** Compound **9s** (cyan) docked into PDB ID: 4BCG, in which the CDK9 adopts a closed conformation around the crystal ligand (orange). **B.** **9q** (green) and **9s** (cyan) adopt similar binding orientations when docked into 4BCG. **C.** **9s** adopts a similar conformation when docked into either a closed (4BCG, cyan) or open (4BCF, magenta) structure of CDK9. Note that the active sites of the open and closed structures are almost identical, except for the position of the glycine rich loop incorporating Thr29. **D.** **9q** adopts a different binding mode in the open (yellow) or closed (green) CDK9 crystal structures, driven by an internal hydrogen bond in the open structure. **E.** Modelled conformations of **9q** (green) and **9s** (cyan) in CDK2 (4BCP). **9q** participates in a water mediated hydrogen bonding network.

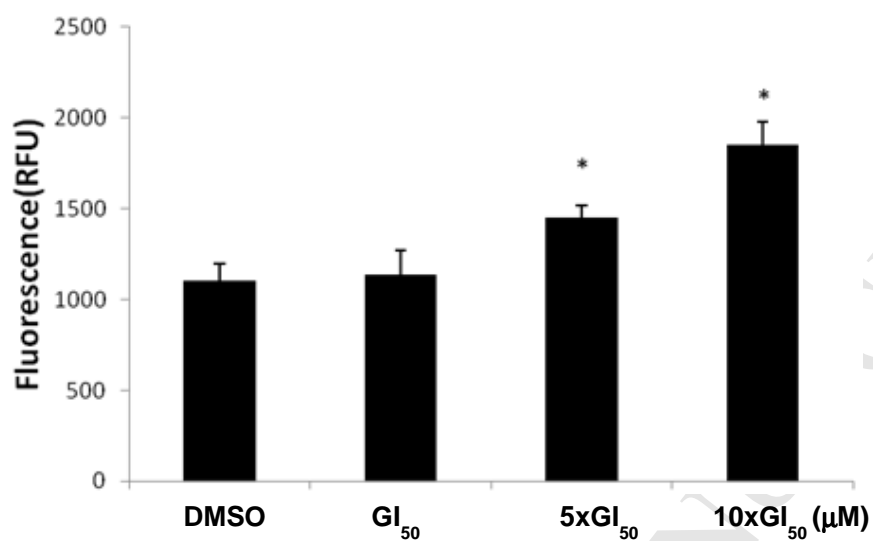


Figure 2 Induction of caspase-3 activity in HCT-116 cells after treatment with **9s** at the GI₅₀, 5× GI₅₀ or 10× GI₅₀ µM for 24 h. Vertical bars represent the mean ± S.D. of three independent experiments. Values significantly ($p < 0.01$) different from DMSO control are marked with an asterisk (*).

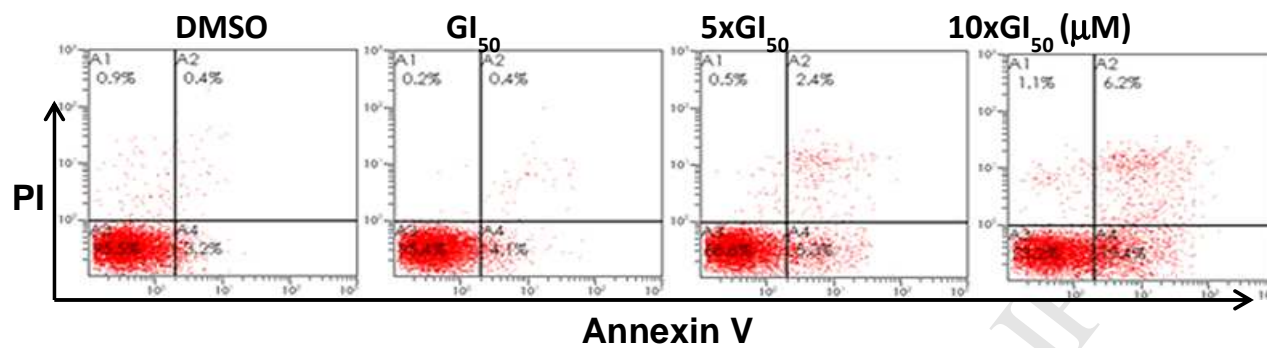


Figure 3 HCT-116 cells were treated with **9s** for 24 h and analysed by annexin V/PI staining. The percentage of cells undergoing apoptosis was defined as the sum of early apoptosis (annexin V-positive cells) and late apoptosis (annexin V-positive and PI-positive cells).

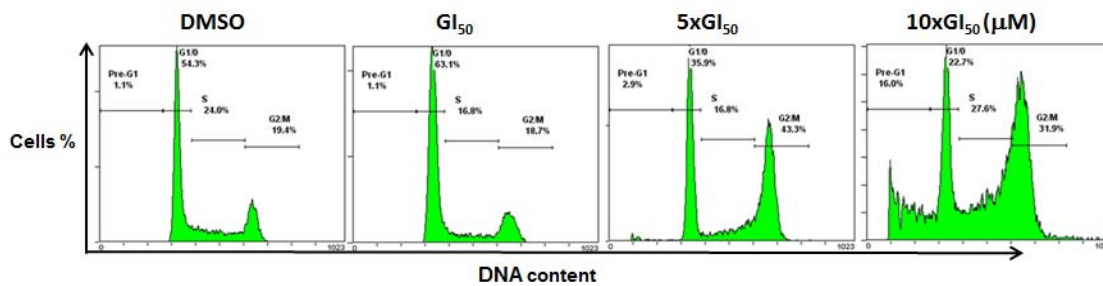


Figure 4 Cell-cycle analysis of HCT-116 cells following treatment with **9s** at the GI_{50} , $5 \times GI_{50}$ or $10 \times GI_{50}$ μM for 24 h.

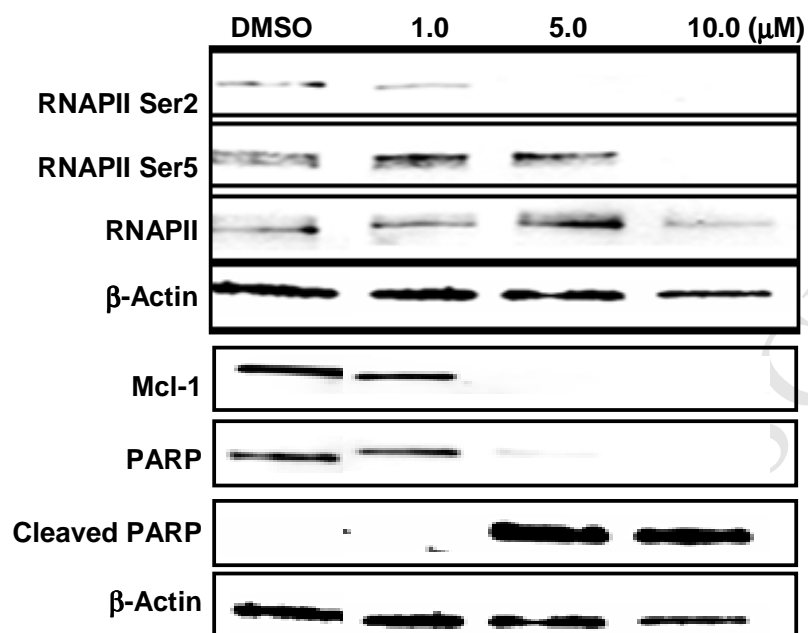


Figure 5 Cellular mode of action of 9s by western blotting analysis: HCT-116 cells were treated with 9s for 24 h at the concentrations shown. β-Actin was used as internal control.

Highlights

- We prepared a series of 2,4,5-trisubstituted pyrimidine compounds.
- They exhibit potent CDK inhibitory and anti-proliferative activities.
- Their structure activity relationships are described.
- **9s** inhibits cellular CDK9 activity and induces cancer cell apoptosis.

Supporting Information

Synthesis, structure-activity relationship and biological evaluation of 2,4,5-trisubstituted pyrimidine CDK inhibitors as potential anti-tumour agents

Hao Shao^a, Shenhua Shi^a, David W. Foley^a, Frankie Lam^{a,b}, Abdullah Y. Abbas^a, Xiangrui Liu^a, Shiliang Huang^a, Xiangrui Jiang^a, Nadiah Baharin^a, Peter M. Fischer^a and Shudong Wang^{a,b*}

^aSchool of Pharmacy and Centre for Biomolecular Sciences, University of Nottingham, Nottingham NG7 2RD, UK

^bSansom Institute for Health Research and School of Pharmacy and Medical Sciences, University of South Australia, Adelaide SA 5001, Australia

*Corresponding author. Sansom Institute for Health Research and School of Pharmacy and Medical Sciences, University of South Australia, Adelaide SA 5001, Australia.

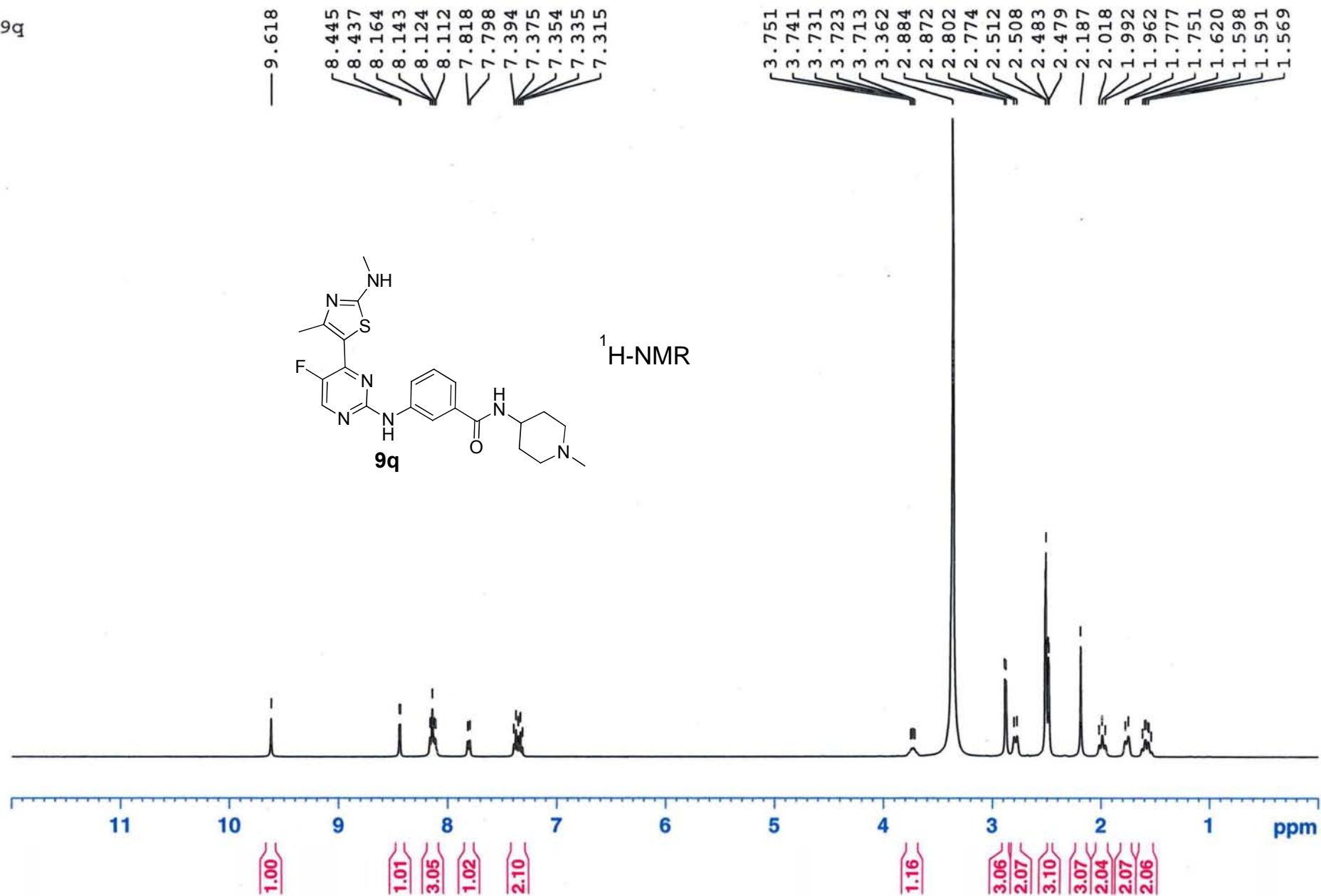
Tel.: +61 883022372; fax: +61 883021087.

E-mail address: shudong.wang@unisa.edu.au (S. Wang).

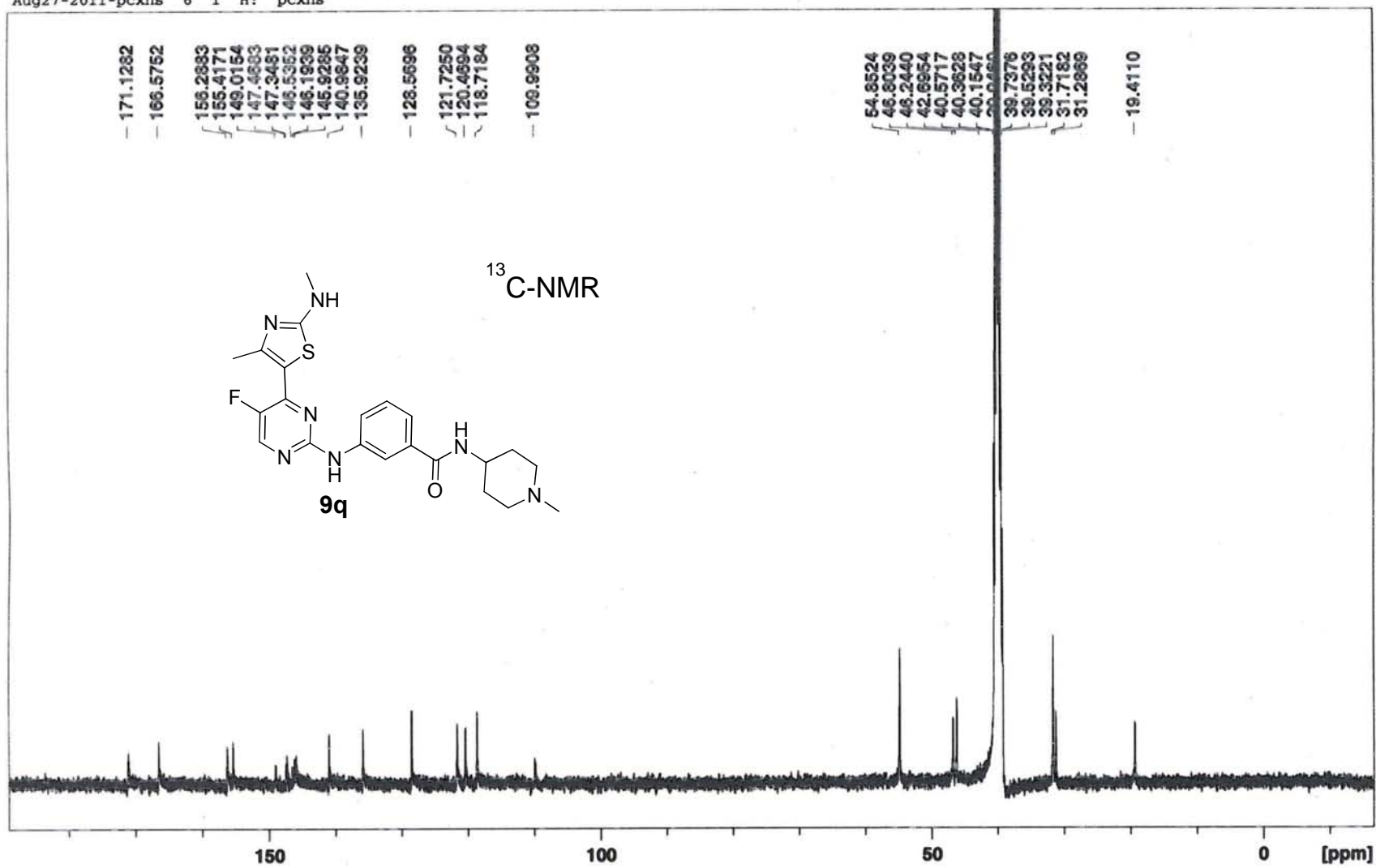
Content

¹H-NMR and ¹³C-NMR spectra of **9q**, **9r** and **9s**.

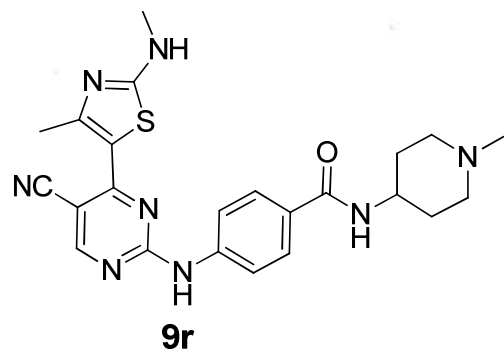
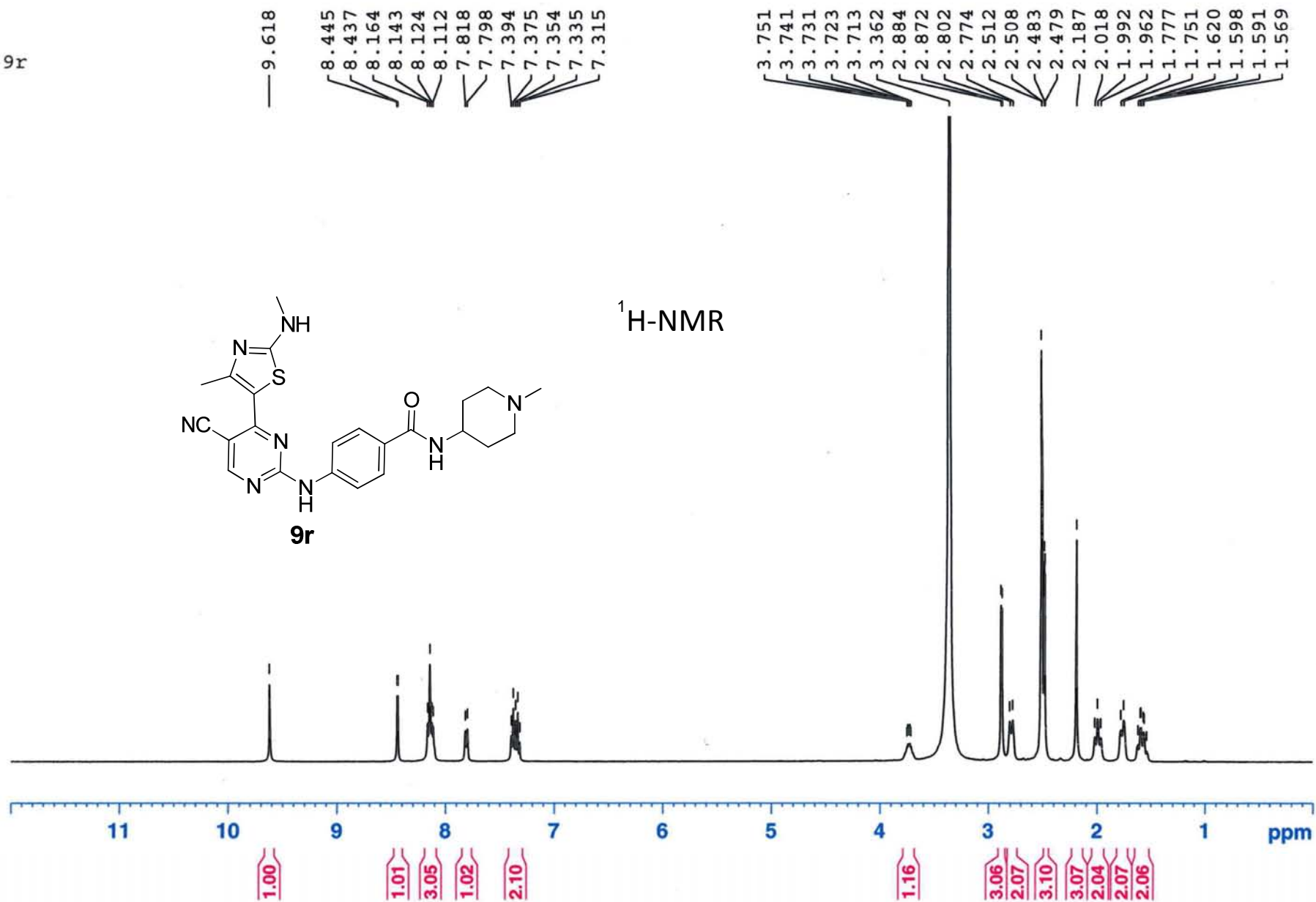
9q

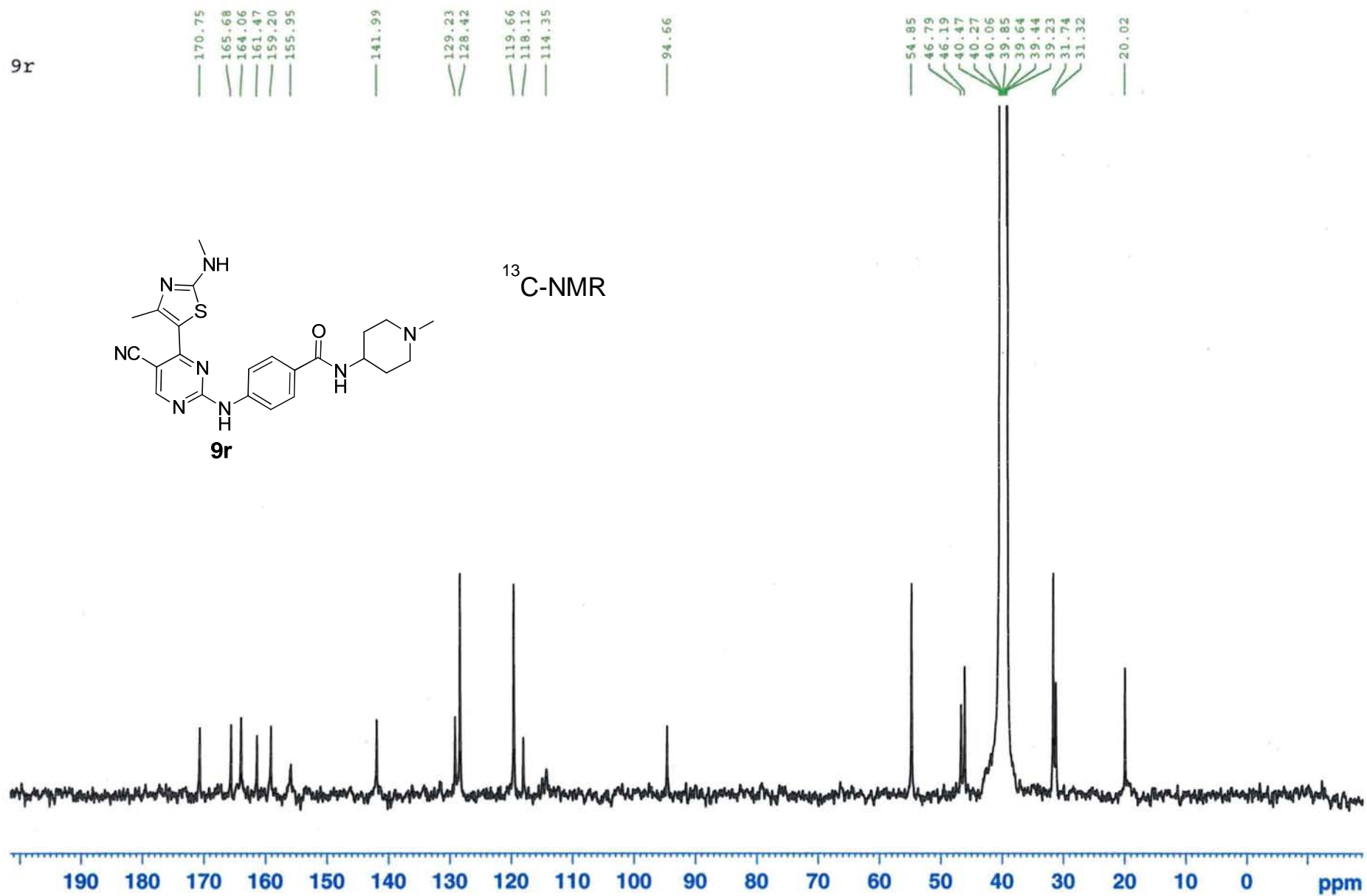


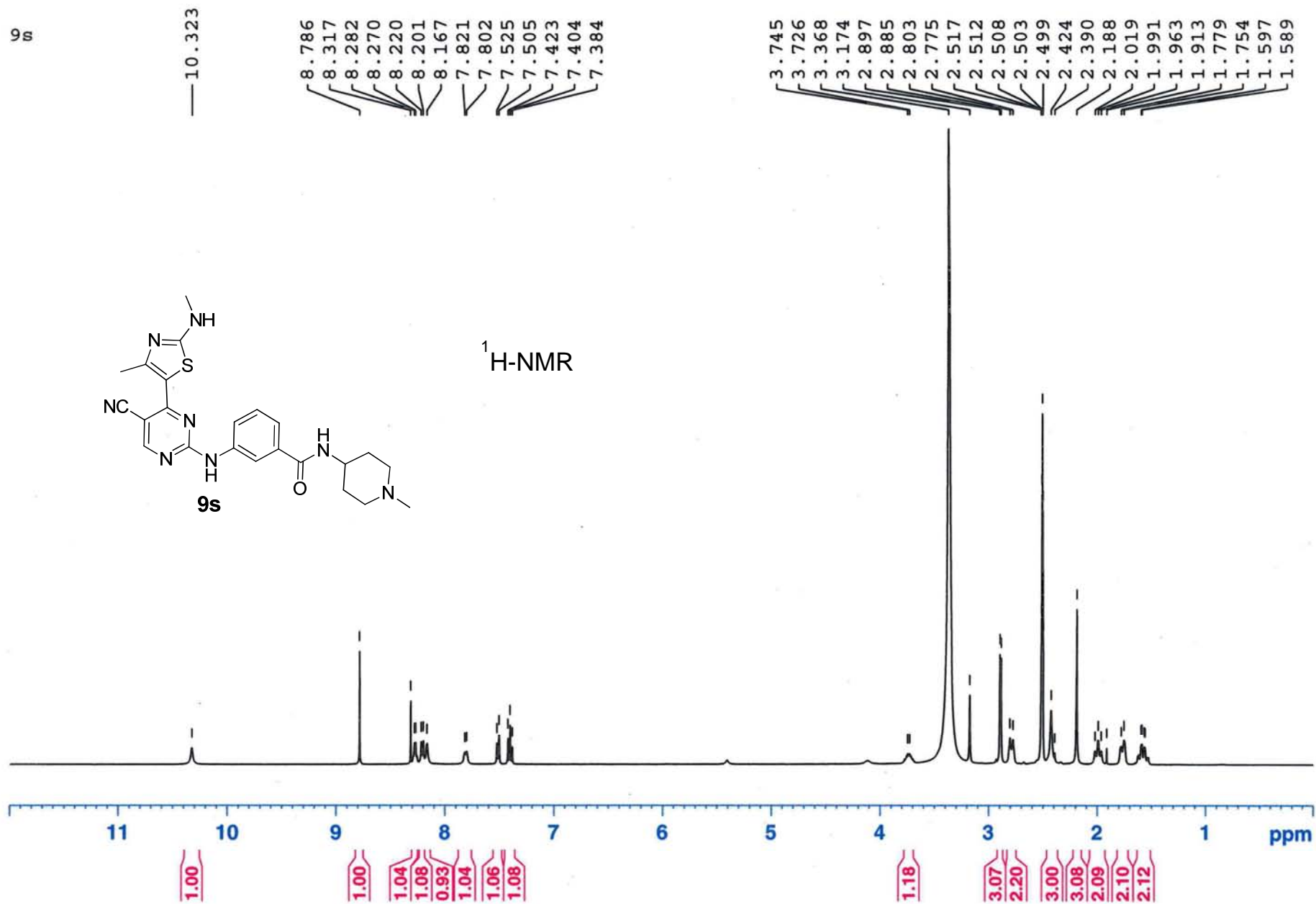
Aug27-2011-pcxhs 6 1 H: pcxhs



9r

¹H-NMR





9S

 ^{13}C -NMR